

SGNet: Folding Symmetrical Protein Complex with Deep Learning

Zhaoqun Li Jingcheng Yu Qiwei Ye

Beijing Academy of Artificial Intelligence

Abstract

Deep learning has made significant progress in protein structure prediction, advancing the development of computational biology. However, despite the high accuracy achieved in predicting single-chain structures, a significant number of large homo-oligomeric assemblies exhibit internal symmetry, posing a major challenge in structure determination. The performances of existing deep learning methods are limited since the symmetrical protein assembly usually has a long sequence, making structural computation infeasible. In addition, multiple identical subunits in symmetrical protein complex cause the issue of supervision ambiguity in label assignment, requiring a consistent structure modeling for the training. To tackle these problems, we propose a protein folding framework called SGNet to model protein-protein interactions in symmetrical assemblies. SGNet conducts feature extraction on a single subunit and generates the whole assembly using our proposed symmetry module, which largely mitigates computational problems caused by sequence length. Thanks to the elaborate design of modeling symmetry consistently, we can model all global symmetry types in quaternary protein structure prediction. Extensive experimental results on a benchmark of symmetrical protein complexes further demonstrate the effectiveness of our method.

1. Introduction

Protein structure prediction is a crucial step in understanding complex protein functionality. The way in which proteins interact with each other provides insight into how biological processes occur at the molecular level [4, 16, 29]. Recent deep learning techniques [3, 8, 10, 11, 14, 20, 25, 26] have been widely applied in this domain, leading to the development of novel drug discovery, protein engineering, protein-ligand binding, and more. AlphaFold [8, 18] has shown promising performance in predicting complex structures; however, predicting the folding of large homo-oligomeric protein complexes remains a major challenge.

A significant category of protein-protein interactions is

formed by homo-oligomers with specific symmetry [9, 21], especially for large protein complexes. For example, virus capsids are typically composed of many identical proteins arranged with icosahedral symmetry. Therefore, modeling and predicting symmetrical protein complexes are critical for understanding the fundamental mechanisms involved in protein folding, shedding light on general multi-chain protein structure prediction. Traditional computational methods typically use symmetry docking algorithms to tackle this problem, such as HSYDOCK [28] and SymDock2 [6]. Unfortunately, the docking process typically suffers from both low accuracy and long latency. Certain recent studies [4, 5, 7, 11, 12, 22] have been able to predict multimeric interfaces and attain promising performance. To overcome the issue of label assignment permutation symmetry in homomeric components, AlphaFold-Multimer (AFM) [8] proposes multi-chain permutation alignment that greedily searches for a good permutation during training. AFM achieves high accuracy in predicting symmetrical structures, yet it faces challenges in terms of residue length restrictions and the greedy search process lacks stability during training of cubic symmetrical complexes. Leveraging the symmetry group property, UF-Symmetry [21] designs a training regime to hasten symmetry complex folding and assemble the entire protein in an end-to-end manner.

Despite numerous efforts devoted to the field, predicting the structure of symmetrical proteins using deep learning remains a challenging problem. The task primarily encounters two major obstacles. Firstly, the sequence of a symmetrical protein assembly is typically very long as it consists of multiple subunits. Popular methods like AFM have cubic complexity and suffer from the notorious sequence length issue, which may cause computational infeasibility. Secondly, another difficulty arises from the symmetrical structure, which brings a label assignment issue in supervised learning. As the subunits are identical sequences, a fully sequence-to-structure model would encounter supervision ambiguity. Therefore, a proper training scheme that considers the symmetry characteristics is also desirable.

To address this gap, we propose a methodology for modeling the symmetrical protein quaternary structure that

leverages protein-protein interface properties and underlying inter-chain relations. By enumerating and analyzing all structural topologies in symmetrical protein assemblies, we unify the symmetry relation representation using relative position maps and design a symmetry generator that can duplicate subunits to reconstruct the whole assembly. All global symmetry types in proteins can be modeled in this approach. Additionally, based on the structure modeling, we propose Symmetry Generator Network (SGNet), which is a neural framework specially designed for symmetrical protein folding. In the framework, the sequence feature extractor is based on evoformers and leverages single-chain feature embedding and geometric information extracted from AFM. The symmetry module takes the pre-trained single-chain feature as input to construct the whole symmetrical protein assembly. In this way, we can largely alleviate the computational problems caused by sequence length. And during the training stage, the learning objectives are modeled consistently to avoid ambiguity issues. Experimental results demonstrate that our framework can model protein symmetry and achieve better performance than the baseline method, AlphaFold-Multimer. The contributions are summarized as follows:

- We develop folding algorithms that specifically model global symmetry in protein complex structure, including Cyclic, Dihedral, Tetrahedral, Octahedral and Icosahedral symmetries.
- We implement a deep model named SGNet for symmetrical protein complex structure prediction leveraging inter-chain interfaces, achieving competitive performance on quaternary structure prediction.

2. Related work

Most protein complexes tend to exhibit symmetry, with multiple identical subunits forming the structure and interacting with neighboring subunits in the same manner. Predicting the whole protein complex structure is challenging since the protein is usually huge. Traditional computational methods typically use symmetry docking algorithms to tackle this problem [6, 23, 24]. HSYDOCK [28] presents a computational tool designed to predict the structure of protein homo-oligomers that have specific types of symmetry, namely cyclic or dihedral. These types of symmetries are common in homo-oligomeric proteins, which are complexes made up of several identical subunits. SymDock2 [6] focuses on a computational method or framework for assembling and refining the three-dimensional structures of symmetrical homomeric complexes, where multiple identical protein subunits assemble in a specific symmetric pattern. Regrettably, the docking process often experiences both limited precision and extended delays.

Certain recent studies [4, 5, 7, 11, 12, 15, 22, 27] have been able to predict multimeric interfaces and attain promis-

ing performance. AlphaFold [8, 18] has demonstrated impressive capabilities in predicting the structures of both monomeric and multimeric proteins; however, it faces constraints related to the count of protein chains and the number of amino acid residues it can process. In [15], authors present a method that combines AlphaFold’s capabilities with all-atom symmetric docking simulations to predict the structure of complex symmetrical protein assemblies. This approach allows for the energetic optimization of models and aids in the study of intermolecular interactions within symmetrical assemblies. RFDiffusion [27] introduces a deep-learning framework for designing proteins, addressing a broad spectrum of design challenges, including the creation of new binders and symmetric structures. The RoseTTAFold structure leads to a generative model for protein backbones with high performance in various design applications. However, the framework is not designed for symmetric structure prediction.

3. Preliminaries

3.1. Symmetry group

The symmetry group of a geometric object is the group of all transformations under which the object is invariant. Oligomeric assemblies can exhibit two categories of symmetries: point group symmetry or helical symmetry [13]. The paper narrows its focus specifically on finite point groups including five types: Cyclic groups (C_n), Dihedral groups (D_n), Tetrahedral group (T), Octahedral group (O) and Icosahedral group (I).

In the first two symmetry symbols, n means the symmetry group has n -fold cyclic axis. Among these symmetry groups, T, O and I symmetries are cubic symmetries which are more challenging to dissolve.

3.2. Backbone frames

We follow [18] to represent one backbone frame via a tuple $T : (R, t) \in \text{SE}(3)$. In the tuple, R is the rotation matrix, t is the translation vector which is also the position of C^α by definition. The backbone of a protein chain with length N can be represented as a sequence $\{T_i\}_{i \leq N}$. Each backbone frame also represents a 3D Euclidean transform from the local frame to a global reference frame:

$$x_{global} = T \circ x_{local} = Rx_{local} + t \quad (1)$$

The composition of two Euclidean transforms is denoted as

$$T_{comp} = T_1 \circ T_2 = (R_1R_2, R_1t_2 + t_1) \quad (2)$$

The relative position of one point $x \in \mathbb{R}^3$ with respect to a coordinate system T is the local coordinate of x in T :

$$x_{local} = T^{-1} \circ x_{global} = R^T(x_{global} - t) \quad (3)$$

For convenience, we use \mathcal{T} to represent all backbone frames in a chain.

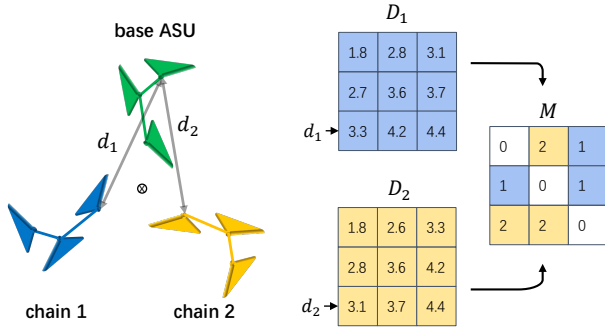


Figure 1. An illustration example of chain index mask generation. \otimes is the symmetry axis.

4. Structural symmetry modeling

In this section, we describe the symmetry modeling from a structural topology view and explain how to formulate the learning objectives. Since residues are basic units of a protein chain, the symmetry structure modeling description solely involves the backbone pose, i.e. \mathcal{T} , and omits the side-chains.

4.1. Protein symmetry

For a symmetrical protein complex, its amino acid sequence is composed of multiple identical subsequences corresponding to identical polypeptide chains. The smallest subsequence is called the asymmetric unit (ASU), and we can also regard it as one protein chain. For example, the protein *Inw4* has D3 symmetry and its sequence is $\{A_1 A_2 A_3 A_4 A_5 A_6\}$, in which each chain A_i is identical to another one and the number of duplicates is 6. We can reconstruct the whole assembly from the ASU if we know its positional relation with its neighboring chains.

Protein contact interface. From a perspective of structural topology [2], there are two types of interfaces between subunits in a symmetry assembly: heterologous interfaces and isologous interfaces. In the topology, ASUs are viewed as graph nodes, and the contact interfaces are the graph edges. Then we can enumerate all quaternary structure topologies in symmetrical protein assembly (see Appendix B). There are various cases in structural topologies, even for one specific symmetry. The intricate cases present a formidable challenge in the field of symmetry modeling when attempting to achieve a satisfactory outcome.

4.2. Relative position map

The symmetric relationship in 3D space can be described by relative position map. Let $\mathcal{T}^a, \mathcal{T}^b$ be the backbone frames of two protein chains in a symmetrical assembly and assume the chain lengths are N_a, N_b . Denote $t^a \in \mathbb{R}^{N_a \times 3}$, $t^b \in \mathbb{R}^{N_b \times 3}$ as the translation vectors. The relative posi-

Algorithm 1 D2 symmetry generator

Input: Backbone frames \mathcal{T} , Confidence score map C , Nearest position map P^{nst} , Chain index map M , Number of selection K , Number of replicates n .

$$\triangleright P^{nst} \in \mathbb{R}^{N \times N}, M \in \mathbb{R}^{7 \times N \times N}, C \in \mathbb{R}^{7 \times N \times N}$$

Output: Atom positions of backbone p_{all} .

$$\triangleright p_{all} \in \mathbb{R}^{n \times N \times 3 \times 3}$$

def D2SymmetryGenerator($\mathcal{T}, P^{nst}, M, C, K, n$)

- 1: $p_{bb} :=$ backbone atom positions $\triangleright p_{bb} \in \mathbb{R}^{N \times 3 \times 3}$
 - 2: $p_0 := C^\alpha$ position $\triangleright p_0 \in \mathbb{R}^{N \times 3}$
 - 3: $S = \text{GetPointIndexSet}(M, C, K)$ $\triangleright S \in \mathbb{R}^{7 \times K \times 2}$
 - 4: $l_1 = \text{SymmetryAxisIsologous}(\mathcal{T}, P^{nst}, S[0])$
 - 5: $l_2 = \text{SymmetryAxisIsologous}(\mathcal{T}, P^{nst}, S[1])$
 - 6: $l_3 = \text{SymmetryAxisIsologous}(\mathcal{T}, P^{nst}, S[2])$
 - 7: $p_1 = \text{ApplySymmetryOp}(p_0, l_1, 2)$
 - 8: $p_2 = \text{ApplySymmetryOp}(p_0, l_2, 2)$
 - 9: $p_3 = \text{ApplySymmetryOp}(p_0, l_3, 2)$
 - 10: $l_1, l_2, l_3 = \text{SymmetryAxisIsosceles}(p_0, p_1, p_2, p_3)$
 - 11: $p_1 = \text{ApplySymmetryOp}(p_{bb}, l_1, 2)$
 - 12: $p_2 = \text{ApplySymmetryOp}(p_{bb}, l_2, 2)$
 - 13: $p_3 = \text{ApplySymmetryOp}(p_{bb}, l_3, 2)$
 - 14: $p_{all} = \text{concat}(p_{bb}, p_1, p_2, p_3)$
 - 15: **return** p_{all}
-

tion map between the two protein chains is defined as the C^α local coordinate map:

$$P_{a,b}^r \in \mathbb{R}^{N_a \times N_b \times 3} \quad (4)$$

$$P_{a,b}^r(i, j) = \mathcal{T}_i^{a-1} \circ t_j^b$$

that is, the pixel (i, j) in the relative position map stores the local coordinate of j -th C^α in chain b with respect to i -th backbone frame \mathcal{T}_i^a . An important property of the representation is that P^r is *SE(3)-invariant*. This can be obtained by applying an arbitrary transformation $T_g \in \text{SE}(3)$ to both chains:

$$\begin{aligned} (T_g \circ \mathcal{T}_i^a)^{-1} \circ (T_g \circ t_j^b) &= \mathcal{T}_i^{a-1} \circ T_g^{-1} \circ T_g \circ t_j^b \\ &= \mathcal{T}_i^{a-1} \circ t_j^b \end{aligned} \quad (5)$$

The isologous/heterologous interfaces can be determined by relative position map and then we can calculate the symmetry axes. We implement empirical algorithms for the calculation, which are described in detail in Appendix (Alg. 6 and Alg. 7).

4.3. Nearest position map and chain index mask

Our goal is to reconstruct the whole symmetrical assembly using relative position maps of ASU. However, learning P^r is not trivial considering the quotient space property. The training should involve permutation invariance in label assignment and in the inference the model should generate

one determined structure. For example, in Fig. 1 the sample has C3 symmetry. The green chain has two equivalent neighbour chains, corresponding two relative position maps P_1^r, P_2^r .

Since all subunits are equivalent in the whole assembly, without loss of generality, we select one subunit as object of study and call it *base ASU*. Under the the assumption that the base ASU only interacts with the nearest residues of neighbor chains, we propose to learn nearest position map:

$$\begin{aligned} M_a(i, j) &= \arg \min_{k \in \mathcal{N}} D_{a,k}(i, j) \\ P^{nst}(i, j) &= P_{a, M_a(i, j)}^r(i, j) \end{aligned} \quad (6)$$

where D is the inter-chain distance matrix defined by pairwise distance of C^α , \mathcal{N} is the index set of neighbour chains of the base ASU a . M indicates the chain index map, as shown in Fig. 1. The neighbour relation is the same as that defined in structural topology. Note that P^{nst} has no subscript of a because it is independent of the choice of base ASU. P^{nst} is a symmetric function with P^r as its variables (P_1^r and P_2^r for the sample in Fig. 1) and thus is *invariant* under label assignment. It also inherits the SE(3)-invariant property from P^r . In addition to P^{nst} , we also need to distinguish chain index map M in the reconstruction. The learning of M is similar to an image segmentation task, where each pixel is assigned to an integer.

4.4. Symmetry operation and symmetry generator

Symmetry operation preserves all the relevant structure of a geometric object. In protein, it means the whole assembly is unchanged after applying one specific rotational transformation. We denote the rotational transformation as $R_\theta^l : \mathbb{R}^3 \rightarrow \mathbb{R}^3$, where $l = [l_s, l_e] \in \mathbb{R}^{2 \times 3}$ is the rotation axis and θ is the rotation angle. Note that a rotation axis is a line without direction, we only use two points on it to represent it to ease the algorithm description. Using the elements in symmetry group, each symmetry type can connect to a function G that generates the whole assembly by duplicating the ASU:

$$\begin{aligned} G : \mathbb{R}^{N \times 3} \times \mathbb{R}^{K \times 2 \times 3} &\rightarrow \mathbb{R}^{N_{all} \times 3} \\ G(x, \{l_i\}) &= x_{all} \end{aligned} \quad (7)$$

In Eq. 7, $N_{all} = n \times N$ and n is the number of replicates, K is the number of rotation axes in the symmetry assembly. We name this function *symmetry generator*. In our method, we implement these symmetry generators and force the functions to output symmetrical protein structure. For instance, in C_n symmetry there is only one n -fold symmetry axis l , and we have:

$$G_{C_n}(x, \{l\}) = \oplus (R_{\theta_1}^l(x), R_{\theta_2}^l(x), \dots, R_{\theta_n}^l(x)) \quad (8)$$

where $\theta_i = \frac{2\pi i}{n}$, $i = 1, 2, \dots, n$ and \oplus is concatenation operation.

As to D symmetry, the situation becomes more complicated. For $n = 3$, three equivalent isologous interfaces need to be considered, corresponding three two-fold symmetry axes l_1, l_2, l_3 . In reality, l_1, l_2, l_3 should intersect at one point while the predicted symmetry axes are not always consistent. We design an algorithm described as pseudo code in Alg. 1. In the algorithm, we leverage pairwise distances of four chains to build a isosceles tetrahedron. Then the ASUs are placed ‘‘appropriately’’ on the vertices of the isosceles tetrahedron. Details of Alg. 1 description and T, O, I symmetry generator implementation are presented in Appendix E.

5. Framework

This section depicts the overall network pipeline and our proposed symmetry module for predicting the protein structure. In the following, we denote the number of residues in the input sequence by N .

5.1. Overview

The overall pipeline is shown in Fig. 2. There are mainly two parts in our framework, the ASU structure prediction module and the proposed symmetry module. From the protein structure model, which is pretrained in protein folding prediction task, we can obtain ASU sequence features and its structure: $s, z, \mathcal{T}, \mathcal{T}_{inter}$. Here, $s \in \mathbb{R}^{N \times C_s}$ is the single representation, $z \in \mathbb{R}^{N \times N \times C_z}$ is the intra-chain pair representation, $\mathcal{T}, \mathcal{T}_{inter}$ are the backbone frames of ASU and its neighbour chains. The symmetry module takes ASU structure and inter-chain pair representation as input, generating the whole assembly:

$$x_{all} = \text{SymmetryModule}(s, z, \mathcal{T}, \mathcal{T}_{inter}) \quad (9)$$

where x_{all} represents all atom positions in backbones of the symmetrical protein assembly.

5.2. Pretrain feature embedding

Before input to the symmetry module, we explicitly extract geometric information from the pretrained protein structure model. The original pair representation z only have intra-chain information. To enhance the inter-chain feature representation, we regard the distance matrix among neighbour chains as a priori knowledge and add it to z :

$$z_{input} = z + \text{Linear}(d_{\mathcal{T}, \mathcal{T}_{inter}}) \quad (10)$$

where d represents inter-chain distance matrix, which is calculated using either 1 or 2 neighbour chains depending on whether interface is isologous or heterologous.

5.3. Symmetry module

The objective of the symmetry module is to reconstruct the whole assembly by using protein-protein interfaces and

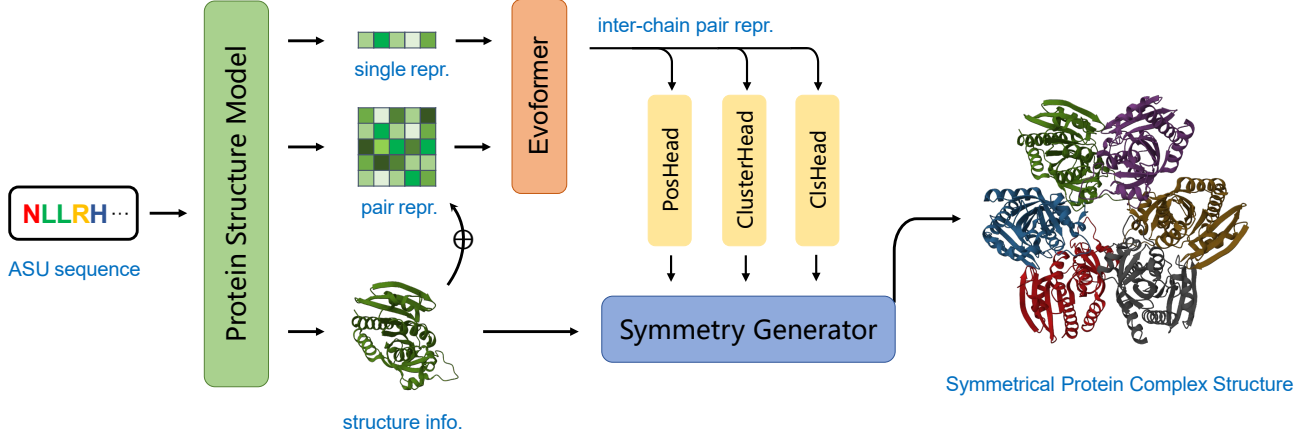


Figure 2. The pipeline of SGNet follows a two-phase, end-to-end process for predicting structure. Initially, the ASU structure is generated using both single and pair representation from a pretrained ASU structure module. Then, the symmetry module expands the ASU to the whole assembly through protein-protein interface information.

symmetry relations. As discussed in Sec. 4.2, our core idea lies in predicting nearest relative position maps, which provide sufficient symmetry information. To achieve this, in the symmetry module, we add an Evoformer stack [18] to further extract inter-chain features for multimeric interface prediction:

$$z_{inter} = \text{Evoformer}(s, z_{input}) \quad (11)$$

The resulted feature $z_{inter} \in \mathbb{R}^{N \times N \times C_z}$ is inter-chain pair representation. After, as shown in Fig. 2, three lightweight heads are added on the top of z_{inter} to learn the desired components (see Appendix D.1 for details of the head architectures).

In a symmetrical assembly, the ASU has at most three isologous interfaces and two heterologous interfaces (see Appendix B). Each isologous interface corresponds one neighbour chain, and each heterologous interface corresponds two neighbour chains, so the ASU has at most seven neighbour chains. PosHead generates the relative position map P^{nst} for both isologous and heterologous interfaces:

$$P^{nst} = \text{PosHead}(z_{inter}) \quad (12)$$

To distinguish which chain each pixel belongs to, ClusterHead predicts chain index segmentation mask:

$$H = \text{ClusterHead}(z_{inter}) \quad (13)$$

where $H \in \mathbb{R}^{N \times N \times 7}$ indicates classification score for each neighbour chain. H also serves as confidence score map in solving symmetry axis. As the symmetry generators differs with symmetry types, we need to predict one specific type of C, D, T, O and I:

$$Y = \text{ClsHead}(z_{inter}) \quad (14)$$

where $Y \in \mathbb{R}^5$ is the symmetry type classification score.

5.4. Loss functions

In this section, we introduce each loss function. The final loss is the linear combination of loss values with loss weight.

Distogram loss. To supervise the learning of z_{inter} , we leverage the distogram loss from AFM that utilizes a linear projection to map the inter-chain pairwise representations z_{inter} onto 64 distance bins. The bin probabilities p_{ij}^b is obtained using softmax operation. The distogram loss is defined as the averaged cross-entropy loss:

$$L_{dist} = -\frac{1}{N^2} \sum_{i,j} \sum_{b=1}^{64} y_{ij}^b \log p_{ij}^b \quad (15)$$

where y_{ij} is the ground truth bin.

Relative position map loss. We assume the atoms has interaction within $d_{clamp} = 20 \text{ \AA}$ distance and only consider close distance interaction. If the distance of two C^α exceeds d_{clamp} , their loss will not be considered. The relative position map error is penalized by an averaged L2-loss:

$$M_v = D^{gt} < d_{clamp} \quad (16)$$

$$L_{pos} = \frac{1}{N^2} \|P^{nst} * M_v - P^{nst,gt} * M_v\|_F$$

Chain index loss. Considering the quotient space property, the desired chain index map M should fulfill the following relationship: $\forall m_i, m_j \in M$, if residues i, j are from the same chain, then $m_i = m_j$. We transfer H to probability by applying softmax $H_p = \text{Softmax}(H) \in \mathbb{R}^{N^2 \times 7}$ and the chain index loss is formulated as:

$$F = (H_p * M_v)(H_p * M_v)^T$$

$$L_{id} = \frac{1}{N^4} \sum_{i,j} (1 - F_{ij}) \cdot F_{ij}^{gt} + F_{ij} \cdot (1 - F_{ij}^{gt}) \quad (17)$$

Symmetry	# Train set	# Test set	Avg. ASU length	Avg. complex length
C	3,000	100	303	778
D	1,000	100	318	1,443
T	200	20	163	1,955
O	200	20	200	4,803
I	150	10	289	17,340

Table 1. Benchmark statistic information.

Model	Dimer		Cyclic _{>2}		Dihedral		Tetrahedral	
	RMSD	TM-score	RMSD	TM-score	RMSD	TM-score	RMSD	TM-score
AlphaFold-Multimer	8.3	0.78	16.3	0.66	10.3	0.77	26.2	0.31
	0.5	-0.04	6.4	0.21	3.2	0.07	21.2	0.61
SGNet	7.8	0.74	9.9	0.87	7.1	0.84	5.1	0.92

Table 2. Performance comparison with AlphaFold-Multimer. The performance gain is displayed in the middle of the table (Best viewed in color).

where the ground truth F_{ij}^{gt} equals to 1 if the chain indexes in pixel i and j are equal. Since optimizing all pairs of chain indexes (N^4 pairs) will encounter memory issue, in practice we instead randomly sample pixels in H and calculate loss on them.

6. Experiments

6.1. Experimental setup

Data and metrics. We provide a symmetrical protein complex benchmark for evaluating our proposed method. The construction of the benchmark is as follows. We retrieved experimentally resolved structural data from the PDB database for protein multimers before 2021-08-01. We filtered all the symmetric protein complexes, and the ground truth symmetry information is collected from the RCSB website¹. Owing to limitation in memory capacity, complexes with the ASU length exceeding 2,000 are excluded in test set. In nature, most protein complexes have C and D symmetry, while a minority possess cubic symmetry. To balance the data distribution of different symmetry types, we randomly select 3,500, 1,100, 220, 220, 160 samples for C, D, T, O and I groups respectively. The statistic information of the benchmark is summarized in Tab. 1. The selected samples are split into train/test set by their release date, *i.e.* the newer samples are in test set. The cutoff date is 2018-04-30 which is consistent with that used in AFM pre-trained model (V1 version) to ensure no information leakage from test set. We utilize Root Mean Squared Deviation (RMSD) and Template-Modeling Score (TM-Score) [30] as

evaluation metrics

Implementation details. Following AlphaFold, multiple sequence alignments and template features are searched and extracted to complement the ASU sequence. Before passing to the network, the input sequences are randomly cropped to 300 residues in the training. The protein structure model is pretrained on monomer prediction task [1]. The symmetry module contains 6 evoformer blocks. It should be noted that symmetry type is optional to input, by default no ground truth symmetry information is provided in the inference stage. Our experiments are conducted on a server with eight Nvidia A100 GPUs, where each GPU has 40 GB memory. The training process consists of 30 epochs. The total batch size is 16. During training, the parameters of the pretrained model are fixed, while the parameters of the symmetry module are learned from scratch.

6.2. Comparison results

Since AlphaFold-Multimer has cubic complexity with sequence length, if the input sequence is very long, it fails on single GPU evaluation due to memory limitation. On the other hand, the computational load of our method mainly depends on the length of the ASU, with SGNet demonstrating the capability to infer across all test set samples. For a fair comparison with AFM, in Tab. 2 we report the performance of samples which are successfully dissolved by AFM on single GPU. The count of successfully resolved samples in the C, D, and T symmetry categories are 72, 69, and 4, respectively. In the table, symmetric dimers extracted from the C symmetry group are itemized separately for a detailed comparison, and the notation > 2 indicates the samples

¹<https://www.rcsb.org/>

Local Metrics	Cyclic	Dihedral	Tetrahedral	Octahedral	Icosahedral	All
RMSD	6.0	5.7	10.6	7.4	15.2	6.8
TM-score	0.76	0.79	0.65	0.84	0.51	0.76

Table 3. Results of SGNet on subsets of different symmetry types.

Symmetry type	Extra ground truth information			Metrics	
	ASU structure	Chain index map	Relative position map	RMSD	TM-score
-	-	-	-	6.8	0.76
✓	-	-	-	6.7	0.76
-	✓	-	-	6.7	0.76
✓	✓	✓	-	5.6	0.77
✓	✓	-	✓	4.1	0.84
✓	✓	✓	✓	0.1	0.96

Table 4. Performance gap analysis.

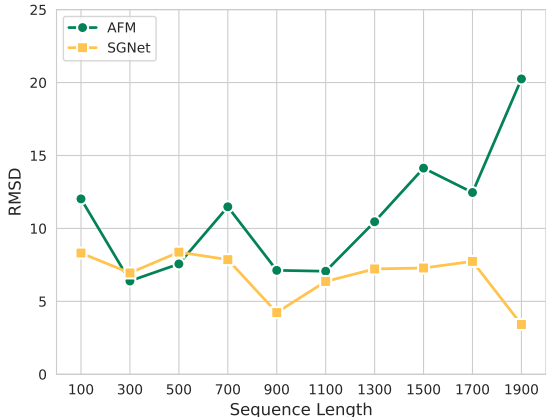


Figure 3. Performance variation with respect to protein length.

comprise more than two monomers. The data presented in the table elucidates that our method outperforms the baseline across all symmetry subsets, while the performance on dimers is comparable. Both methods exhibit proficiency in generating accurate symmetric assemblies with sequences of relatively modest length. However, AFM’s prediction accuracy for cubic symmetry is markedly deficient. In contrast, SGNet shows promise in predicting cubic symmetry within longer sequences, particularly for exceedingly large protein complexes.

6.3. Influence of protein sequence length

Protein sequence length is one crucial factor that influences the structure prediction accuracy of AFM. This assertion could be further corroborated within the realm of symmetric protein prediction. In the Fig. 3, we depict the RMSD value variance with respect to sequence length. To make the plot clearer, we divide the data into several bins based on

sequence length and calculate the average RMSD for each group. The figure shows that SGNet is more robust to the protein length change, thanks to our two-stage generation process.

6.4. Full evaluation of SGNet

As mentioned before, proteins with cubic symmetries are usually very large. Render their full-scale evaluation is challenging, if not unfeasible, particularly when we consider all atoms and all chain permutations. To ease the metric computation, we restrict our evaluation to a select subset of monomers that are essential for constituting the complete assembly (e.g. for icosahedra, the subunits at the five-fold, three-fold, and two-fold symmetry axes) to reduce the computational cost [27]. Concretely, the local subset comprises 2, 3, 4, 4, 5, and 6 monomers for symmetries C_2 , C_n , D_n , T , O , and I , respectively. It should be noted the local metrics and global metrics are consistent in assessing the quality of predicted proteins. This strict correlation comes from the perfect symmetry in our output protein complexes. The full evaluation results on the test set of our method are presented in Tab. 3, where the metrics are calculated locally. We show some cases in Fig. 4. From the results we could conclude that our method performance well on C and D symmetry. However, the construction of cubic symmetry remains a formidable challenge, primarily due to the necessity of inferring multiple interfaces, which makes it more sensitive to possible errors in head prediction.

6.5. Ablation study

To investigate the performance gap and analyze the effectiveness of the components in symmetry module, we replace some of the predicted outputs with the actual ground truth values and then look at how this affect the structures. The evaluation results are shown in Tab. 4. The first three rows

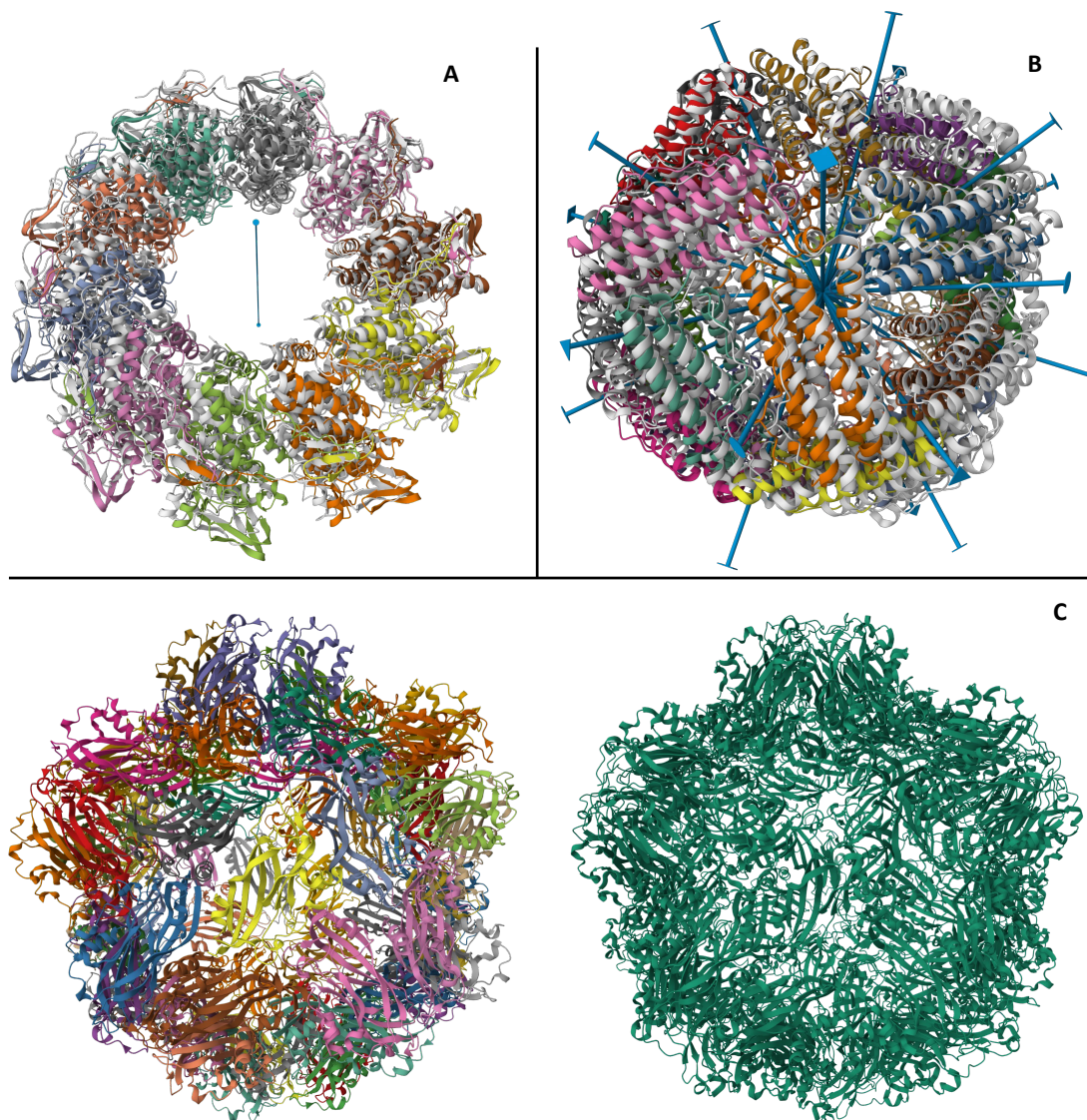


Figure 4. (A) and (B) are protein superimposition where the blue symmetry axes are also rendered. In (C) we place the ground truth on right for better visualization. (A) 2qvj, C10 symmetry. (B) 5xx9, O symmetry. (C) 5yl1, I symmetry.

of the table show that correctly predicting the ASU structure and the type of symmetry have little effect on the overall performance, suggesting these parts of our method are learned well. In fact, the chain index head and relative position map are more important since they are directly related to geometric information, and they are harder to predict accurately. The last row of the table, where we replaced everything with ground truth values, shows the systematic error of our framework in the implementation.

7. Conclusion

Most large proteins exhibit symmetry in their structure. In this paper, our aim is to investigate protein–protein interac-

tions within symmetry assemblies and present an effective framework, SGNet, for predicting symmetrical protein folding. Our main focus is on modeling symmetrical structures and we accomplish this by proposing the use of a relative position map to streamline the representation of symmetry relations. Through careful modeling of symmetry, our framework can capture all global symmetry types in predicting quaternary protein structures. Additionally, SGNet conducts feature extraction on a single subunit and leverages our proposed symmetry module to generate the entire assembly. This approach greatly reduces the computational complexity caused by lengthy sequences. Our future work will focus on improving performance of structure prediction for cubic symmetry.

References

- [1] Gustaf Ahdriz, Nazim Bouatta, Sachin Kadyan, Qinghui Xia, William Gerecke, Timothy J O'Donnell, Daniel Berenberg, Ian Fisk, Niccolò Zanichelli, Bo Zhang, Arkadiusz Nowaczynski, Bei Wang, Marta M Stepniewska-Dziubinska, Shang Zhang, Adegoke Ojewole, Murat Efe Guney, Stella Biderman, Andrew M Watkins, Stephen Ra, Pablo Ribalta Lorenzo, Lucas Nivon, Brian Weitzner, Yih-En Andrew Ban, Peter K Sorger, Emad Mostaque, Zhao Zhang, Richard Bonneau, and Mohammed AlQuraishi. Openfold: Retraining alphafold2 yields new insights into its learning mechanisms and capacity for generalization. *bioRxiv*, 2022.
- [2] Sebastian E Ahnert, Joseph A Marsh, Helena Hernández, Carol V Robinson, and Sarah A Teichmann. Principles of assembly reveal a periodic table of protein complexes. *Science*, 2015.
- [3] Minkyung Baek, Frank DiMaio, Ivan Anishchenko, Justas Dauparas, Sergey Ovchinnikov, Gyu Rie Lee, Jue Wang, Qian Cong, Lisa N Kinch, R Dustin Schaeffer, et al. Accurate prediction of protein structures and interactions using a three-track neural network. *Science*, 2021.
- [4] Patrick Bryant, Gabriele Pozzati, and Arne Elofsson. Improved prediction of protein-protein interactions using alphafold2. *Nature communications*, 2022.
- [5] Patrick Bryant, Gabriele Pozzati, Wensi Zhu, Aditi Shenoy, Petras Kundrotas, and Arne Elofsson. Predicting the structure of large protein complexes using alphafold and monte carlo tree search. *Nature Communications*, 2022.
- [6] Shourya S Roy Burman, Remy A Yovanno, and Jeffrey J Gray. Flexible backbone assembly and refinement of symmetrical homomeric complexes. *Structure*, 2019.
- [7] Bo Chen, Ziwei Xie, Jiezhong Qiu, Zhaofeng Ye, Jinbo Xu, and Jie Tang. Improved the protein complex prediction with protein language models. *BioRxiv*, 2022.
- [8] Richard Evans, Michael O'Neill, Alexander Pritzel, Natasha Antropova, Andrew Senior, Tim Green, Augustin Židek, Russ Bates, Sam Blackwell, Jason Yim, Olaf Ronneberger, Sebastian Bodenstern, Michal Zielinski, Alex Bridgland, Anna Potapenko, Andrew Cowie, Kathryn Tunyasuvunakool, Rishub Jain, Ellen Clancy, Pushmeet Kohli, John Jumper, and Demis Hassabis. Protein complex prediction with alphafold-multimer. *bioRxiv*, 2021.
- [9] Aljaž Gaber and Miha Pavšič. Modeling and structure determination of homo-oligomeric proteins: An overview of challenges and current approaches. *International journal of molecular sciences*, 2021.
- [10] Octavian-Eugen Ganea, Xinyuan Huang, Charlotte Bunne, Yatao Bian, Regina Barzilay, Tommi Jaakkola, and Andreas Krause. Independent se (3)-equivariant models for end-to-end rigid protein docking. *arXiv preprint arXiv:2111.07786*, 2021.
- [11] Mu Gao, Davi Nakajima An, Jerry M Parks, and Jeffrey Skolnick. Af2complex predicts direct physical interactions in multimeric proteins with deep learning. *Nature communications*, 2022.
- [12] Usman Ghani, Israel Desta, Akhil Jindal, Omeir Khan, George Jones, Nasser Hashemi, Sergey Kotelnikov, Dzmitry Padhorny, Sandor Vajda, and Dima Kozakov. Improved docking of protein models by a combination of alphafold2 and cluspro. *BioRxiv*, 2022.
- [13] David S. Goodsell and Arthur J. Olson. Structural symmetry and protein function. *Annual Review of Biophysics and Biomolecular Structure*, 2000.
- [14] Yinan Huang, Xingang Peng, Jianzhu Ma, and Muhan Zhang. 3dlinker: An e(3) equivariant variational autoencoder for molecular linker design. In *ICML*, 2022.
- [15] Mads Jeppesen and Ingemar André. Accurate prediction of protein assembly structure by combining alphafold and symmetrical docking. *bioRxiv*, 2023.
- [16] Wengong Jin, Jeremy Wohlwend, Regina Barzilay, and Tommi S. Jaakkola. Iterative refinement graph neural network for antibody sequence-structure co-design. In *ICLR*, 2022.
- [17] Marcus Johansson and Valera Veryazov. Automatic procedure for generating symmetry adapted wavefunctions. *Journal of Cheminformatics*, 2017.
- [18] John Jumper, Richard Evans, Alexander Pritzel, Tim Green, Michael Figurnov, Olaf Ronneberger, Kathryn Tunyasuvunakool, Russ Bates, Augustin Židek, Anna Potapenko, et al. Highly accurate protein structure prediction with alphafold. *Nature*, 2021.
- [19] Wolfgang Kabsch. A solution for the best rotation to relate two sets of vectors. *Acta Crystallographica Section A: Crystal Physics, Diffraction, Theoretical and General Crystallography*, 1976.
- [20] Lucien F Krapp, Luciano A Abriata, Fabio Cortés Rodríguez, and Matteo Dal Peraro. Pesto: parameter-free geometric deep learning for accurate prediction of protein binding interfaces. *Nature Communications*, 2023.
- [21] Ziyao Li, Shuwen Yang, Xuyang Liu, Weijie Chen, Han Wen, Fan Shen, Guolin Ke, and Linfeng Zhang. Uni-fold symmetry: harnessing symmetry in folding large protein complexes. *bioRxiv*, 2022.
- [22] Milot Mirdita, Konstantin Schütze, Yoshitaka Moriwaki, Lim Heo, Sergey Ovchinnikov, and Martin Steinegger. Colabfold: making protein folding accessible to all. *Nature Methods*, 2022.
- [23] Taeyong Park, Minkyung Baek, Hasup Lee, and Chaok Seok. Galaxytongdock: Symmetric and asymmetric ab initio protein-protein docking web server with improved energy parameters. *Journal of Computational Chemistry*, 2019.
- [24] David W Ritchie and Sergei Grudin. Spherical polar fourier assembly of protein complexes with arbitrary point group symmetry. *Journal of Applied Crystallography*, 2016.
- [25] Hannes Stärk, Octavian Ganea, Lagnajit Pattanaik, Regina Barzilay, and Tommi Jaakkola. Equibind: Geometric deep learning for drug binding structure prediction. In *ICML*, 2022.
- [26] Tomer Tsaban, Julia K Varga, Orly Avraham, Ziv Ben-Aharon, Alisa Khramushin, and Ora Schueler-Furman. Harnessing protein folding neural networks for peptide-protein docking. *Nature communications*, 2022.
- [27] Joseph L Watson, David Juergens, Nathaniel R Bennett, Brian L Trippe, Jason Yim, Helen E Eisenach, Woody Ahern, Andrew J Borst, Robert J Ragotte, Lukas F Milles, et al.

De novo design of protein structure and function with rfdiffusion. *Nature*, 620(7976):1089–1100, 2023.

- [28] Yumeng Yan, Huanyu Tao, and Sheng-You Huang. Hsymdock: a docking web server for predicting the structure of protein homo-oligomers with cn or dn symmetry. *Nucleic acids research*, 2018.
- [29] Hong Zeng, Sheng Wang, Tianming Zhou, Feifeng Zhao, Xiufeng Li, Qing Wu, and Jinbo Xu. Complexcontact: a web server for inter-protein contact prediction using deep learning. *Nucleic acids research*, 2018.
- [30] Yang Zhang and Jeffrey Skolnick. Scoring function for automated assessment of protein structure template quality. *Proteins: Structure, Function, and Bioinformatics*, 2004.

Table 5. Structural topologies.

Symmetry Type	Isologous	Heterologous	remark on n
C	1	0	$n = 2$
C	0	1	$n > 2$
D	3	0	$n = 4$
D	1	1	$n > 4$
D	2	1	$n > 4$
T	0	2	$n \geq 12$
T	1	2	$n \geq 12$
T	1	1	$n \geq 12$
O	0	2	$n \geq 24$
O	1	2	$n \geq 24$
O	1	1	$n \geq 24$
I	0	2	$n \geq 60$
I	1	2	$n \geq 60$
I	1	1	$n \geq 60$

Appendix

A. Asymmetric units

The asymmetric unit (ASU) is the smallest portion of a protein assembly structure to which symmetry operations can be applied in order to generate the complete structure. ASU is composed of several protein chains in the assembly and can be determined directly from the input sequence [17]. For instance, the subunit of a sample with sequence $\{A_1A_2A_3A_4B_1B_2\}$ is $\{A_1A_2B_1\}$.

B. Structural topology

We list all cases of structural topologies in Tab. 5. It should be noted that real protein complexes can have more interfaces [2] compared to our modeling. However, it is possible to establish a direct correlation between actual protein structures and the aforementioned idealized modelling by regarding certain weaker inter-subunit contacts as circumstantial.

For the two subunits of one interface, their relative distance maps $D_{1,2}, D_{2,1} \in \mathbb{R}^{N \times N}$ satisfy following properties:

- Isologous: $D_{1,2} = D_{2,1}$, $D_{1,2}$ is a symmetric matrix
- Heterologous: $D_{1,2}^T = D_{2,1}$, $D_{1,2}$ is not symmetric

C. Quotient space property

The symmetric property poses an inevitable issue to the label assignment since it is not unique. Specifically, swapping the index between any two target positions will still lead to a valid assignment and a identical multimer structure. That is to say, the label assignment is permutation invariant which is referred to the quotient space property. Instead of using implicit positional encoding [8], we explicitly address the

problem by modeling symmetry.

D. Implementation details

D.1. Network architecture

PosHead and ClusterHead have same architecture which consists of one residual structure. The channels are the same as input tensor z_{inter} which is 128 for our implementation. ClsHead is a CNN that predicts a classification score over 5 possible symmetry types. The channels of two convolution layers are 128 and 64. The architectures are plotted in Fig. 5.

D.2. Training and inference

The channels of single representation and pair representation are 384 and 128 respectively. The number of selection is 30 in the symmetry generator. The total loss is the linear combination of loss values with loss weights:

$$L = \lambda_1 L_{pos} + \lambda_2 L_{dist} + \lambda_3 L_{id} + \lambda_4 L_{cls} \quad (18)$$

We use Adam optimizer with $\beta_1 = 0.9, \beta_2 = 0.999$ to optimize the network. Regarding the loss weights, $\lambda_{1 \sim 4}$ are 0.5, 0.3, 0.3, 0.1 respectively. The learning rate warms up from 0 to 1e-3 for the first 1,000 steps. After that, the learning rate decays by 5% every 5,000 steps.

E. Symmetry generator

In this section, we provide Python pseudo code for all symmetry generators. We force the output structure to be strictly symmetrical and consider different cases. For example, one heterologous interface plus isologous interface are sufficient to reconstruct the whole assembly for D symmetry. If a protein complex has one heterologous interface and two isologous interfaces, then we choose the isologous interface

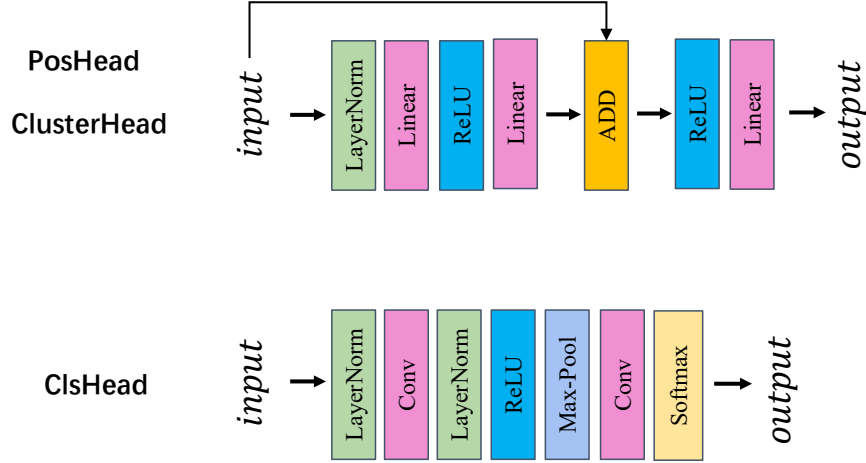


Figure 5. Neural architecture of heads.

which has more contact points to calculate the symmetry axis. For reconstructing neighbour chains by contact interfaces, we adopt Kabsch algorithm [19].

Algorithm 2 Construct local frame from 3 points

Input: Three points $x_1, x_2, x_3 \in \mathbb{R}^3$.

Output: Local frame $T \in \text{SE}(3)$.

def Frame3Points(x_1, x_2, x_3)

- 1: $v_1 = x_3 - x_2$
 - 2: $v_2 = x_1 - x_2$
 - 3: $e_1 = \frac{v_1}{\|v_1\|}$
 - 4: $u_2 = v_2 - e_1(e_1^T v_2)$
 - 5: $e_2 = \frac{u_2}{\|u_2\|}$
 - 6: $e_3 = e_1 \times e_2$
 - 7: $R = \text{concat}(e_1, e_2, e_3)$ $\triangleright R \in \mathbb{R}^{3 \times 3}$
 - 8: $t = x_2$
 - 9: $T = (R, t)$
 - 10: **return** T
-

Algorithm 3 Calculate the vector from a point to a line

Input: $p \in \mathbb{R}^3, l \in \mathbb{R}^{2 \times 3}$.

Output: $v \in \mathbb{R}^3$.

def VecPoint2Line(p, l)

- 1: $s, e = l$
 - 2: $s = s - p$
 - 3: $e = e - p$
 - 4: $v_1 = e - s$
 - 5: $k = -\frac{s^T v_1}{\|v_1\|^2}$
 - 6: $v = s + k v_1$
 - 7: **return** v
-

Algorithm 4 Apply rotational symmetry operation

Input: Point set p , Symmetry axis l , Symmetry order n .

$\triangleright p \in \mathbb{R}^{N \times 3}, l \in \mathbb{R}^{2 \times 3}, n \in \mathbb{N}$

Output: All atom positions p_{all} .

$\triangleright p_{all} \in \mathbb{R}^{n \times N \times 3}$

def ApplySymmetryOp(p, l, n)

- 1: $v = \text{VecPoint2Line}([0, 0, 0], l)$
 - 2: $p = p - v$
 - 3: $l_n = \frac{l[0] - l[1]}{\|l[0] - l[1]\|}$
 - 4: $l_x, l_y, l_z = l_n$
 - 5: $C = \begin{bmatrix} 0 & -l_z & l_y \\ l_z & 0 & -l_x \\ -l_y & l_x & 0 \end{bmatrix}$
 - 6: **for** $i \in \{0, 1, \dots, n-1\}$ **do**
 - 7: $\theta = \frac{2\pi i}{n}$
 - 8: $R = \begin{bmatrix} 1 & 0 & 0 \\ 0 & 1 & 0 \\ 0 & 0 & 1 \end{bmatrix} + (\sin \theta)C + (1 - \cos \theta)C^T C$
 - 9: $p_i = R p$
 - 10: $p_i = p_i + v$
 - 11: **return** p_{all}
-

Algorithm 5 Reconstruct neighbour chain

Input: Backbone frames \mathcal{T} , Relative position map P^r ,
Point index set S .

$$\triangleright \mathcal{T} \in \mathbb{R}^{N \times 4 \times 4}, P^r \in \mathbb{R}^{N \times N \times 3}, S \in \mathbb{R}^{K \times 2}$$

Output: C^α coordinate of the neighbour chain p .

$$\triangleright p \in \mathbb{R}^{N \times 3}$$

def ReconstructNeighbourChain(\mathcal{T} , P^r , S)

```
1:  $K = \text{len}(S)$ 
2: for  $i \in \{0, 1, \dots, K - 1\}$  do
3:    $s, e = S[i]$ 
4:    $T_s = \mathcal{T}[s]$ 
5:    $T_e = \mathcal{T}[e]$ 
6:    $x_i = T_s \circ P^r[s, e]$   $\triangleright x_i \in \mathbb{R}^3$ 
7:    $y_i = T_e.t$   $\triangleright y_i \in \mathbb{R}^3$ 
8: Solve  $T^* = \min_T \sum_i \|y_i - T \circ x_i\|$  by Kabsch algorithm
9: for  $i \in \{0, 1, 2, \dots, N - 1\}$  do
10:   $p[i] = T^* \circ T_i.t$ 
11: return  $p$ 
```

Algorithm 6 Calculate symmetry axis of isologous interface

Input: Backbone frames \mathcal{T} , Relative position map P^r ,
Point index set S .

$$\triangleright \mathcal{T} \in \mathbb{R}^{N \times 4 \times 4}, P^r \in \mathbb{R}^{N \times N \times 3}, S \in \mathbb{R}^{K \times 2}$$

Output: Symmetry axis l .

$$\triangleright l \in \mathbb{R}^{2 \times 3}$$

def SymmetryAxisIsologous(\mathcal{T} , P^r , S)

```
1:  $K = \text{len}(S)$ 
2: for  $i \in \{0, 1, \dots, K - 1\}$  do
3:    $s, e = S[i]$ 
4:    $T_s = \mathcal{T}[s]$ 
5:    $T_e = \mathcal{T}[e]$ 
6:    $x_i = T_s \circ P^r[s, e]$   $\triangleright x_i \in \mathbb{R}^3$ 
7:    $y_i = T_e.t$   $\triangleright y_i \in \mathbb{R}^3$ 
8:    $m_i = \frac{x_i + y_i}{2}$ 
9: Solve  $l = \min_{l'} \sum_i \text{dist}(l', m_i)$  by least square algorithm.
10: return  $l$ 
```

Algorithm 7 Calculate symmetry axis of heterologous interface

Input: C^α coordinate of base ASU p_1 , C^α coordinate of
neighbour chains p_2, p_3 , Number of replicates n .

$$\triangleright p_1, p_2, p_3 \in \mathbb{R}^{N \times 3}$$

Output: Symmetry axis l .

$$\triangleright l \in \mathbb{R}^{2 \times 3}$$

def SymmetryAxisHeterologous(p_1, p_2, p_3)

```
1:  $c_1 = \text{mean}(p_1)$   $\triangleright c_1 \in \mathbb{R}^3$ 
2:  $c_2 = \text{mean}(p_2)$   $\triangleright c_2 \in \mathbb{R}^3$ 
3:  $c_3 = \text{mean}(p_3)$   $\triangleright c_3 \in \mathbb{R}^3$ 
4: if  $n == 3$  then
5:    $\theta_{rot} = \pi - \frac{2\pi}{n}$ 
6: else
7:    $\theta_{rot} = \frac{2\pi}{n}$ 
8:  $T_{rot} = \text{Frame3Points}(c_2, c_1, c_3)$ 
9:  $c_{2,local} = T_{rot}^{-1} \circ c_2$ 
10:  $c_{3,local} = T_{rot}^{-1} \circ c_3$ 
11:  $d_p = c_{3,local} - c_{2,local}$ 
12:  $r = \frac{\|d_p\|}{2 \sin(\theta_{rot})}$ 
13:  $d_{o1} = [-d_p[1], d_p[0]]$   $\triangleright d_{o1}^T d_p = 0$ 
14:  $d_{o2} = [d_p[1], -d_p[0]]$   $\triangleright d_{o2}^T d_p = 0$ 
15: if  $c_{3,local}^T d_{o1} > 0$  then
16:    $d_o = \frac{d_{o1}}{\|d_{o1}\|}$ 
17: else
18:    $d_o = \frac{d_{o2}}{\|d_{o2}\|}$ 
19:  $o_{local} = r d_o$ 
20:  $z_{local} = [0, 0, 1]$ 
21:  $o = T_{rot} \circ o_{local}$ 
22:  $z = T_{rot} \circ z_{local}$ 
23:  $l = [o, z]$ 
24: return  $l$ 
```

Algorithm 8 Select anchor points for reconstructing neighbour chain

Input: Chain id map M , confidence score map C , Number
of selection K .

$$\triangleright M \in \mathbb{R}^{7 \times N \times N}, C \in \mathbb{R}^{7 \times N \times N}$$

Output: Point index set S .

$$\triangleright S \in \mathbb{R}^{7 \times K \times 2}$$

def GetPointIndexSet(M, C, K)

```
1:  $M_{value} = [1, 2, 3, 1, 2, 1, 2]$ 
2: for  $i \in \{0, 1, 2, 3, 4, 5, 6\}$  do
3:    $m_{valid} = M[i] == M_{value}[i]$ 
4:    $C[i][\sim m_{valid}] = +\infty$ 
5:    $idx = \arg \max_i C[i]$ 
6:    $S[i] = idx[: K]$ 
7: return  $S$ 
```

Algorithm 9 Cyclic symmetry generator

Input: Backbone frames \mathcal{T} , Confidence score map C ,
Nearest position map P^{nst} , Chain id map M , Number
of selection K , Number of replicates n .

$\triangleright P^{nst} \in \mathbb{R}^{N \times N}$, $M \in \mathbb{R}^{7 \times N \times N}$, $C \in \mathbb{R}^{7 \times N \times N}$

Output: Atom positions of backbone p_{all} .

$\triangleright p_{all} \in \mathbb{R}^{n \times N \times 3 \times 3}$

def CyclicSymmetryGenerator(\mathcal{T} , P^{nst} , M , C , K , n)

1: $p_{bb} :=$ backbone atom positions $\triangleright p_{bb} \in \mathbb{R}^{N \times 3 \times 3}$

2: $p_0 := C^\alpha$ position $\triangleright p_0 \in \mathbb{R}^{N \times 3}$

3: $S =$ GetPointIndexSet(M , C , K) $\triangleright S \in \mathbb{R}^{7 \times K \times 2}$

4: **if** $n == 2$ **then**

5: $l =$ SymmetryAxisIsologous(\mathcal{T} , P^{nst} , $S[0]$)

6: $p_{all} =$ ApplySymmetryOp(p_0 , l , 2)

7: **else**

8: $p_1 =$ ReconstructNeighbourChain(\mathcal{T} , P^{nst} , $S[3]$)

9: $p_2 =$ ReconstructNeighbourChain(\mathcal{T} , P^{nst} , $S[4]$)

10: $l =$ SymmetryAxisHeterologous(p_0 , p_1 , p_2)

11: $p_{all} =$ ApplySymmetryOp(p_{bb} , l , n)

12: **return** p_{all}

Algorithm 10 Make predicted symmetry axes consistent in D2 symmetry

Input: C^α coordinate of base ASU p_0 , C^α coordinate of neighbour chains p_1, p_2, p_3 .

$\triangleright p_1, p_2, p_3 \in \mathbb{R}^{N \times 3}$

Output: Symmetry axes l_1, l_2, l_3 .

$\triangleright l_1, l_2, l_3 \in \mathbb{R}^{2 \times 3}$

def SymmetryAxisIsosceles(p_0, p_1, p_2, p_3)

1: $O = \text{mean}(p_0)$

2: $A = \text{mean}(p_1)$

3: $B = \text{mean}(p_2)$

4: $C = \text{mean}(p_3)$

5: $x_{neg} = O + O - B$

6: $T_g = \text{Frame3Points}(x_{neg}, O, A)$

7: $OA = \frac{\|O-A\| + \|B-C\|}{2}$

8: $OB = \frac{\|O-B\| + \|A-C\|}{2}$

9: $OC = \frac{\|O-C\| + \|A-B\|}{2}$

10: $a_2 = OA^2$

11: $b_2 = OB^2$

12: $c_2 = OC^2$

\triangleright Solve tetrahedron volume and triangle area by Heron's formula

13: $V = \sqrt{(a_2 + b_2 - c_2)(a_2 - b_2 + c_2)(-a_2 + b_2 + c_2)/72}$

14: $S = \sqrt{(OA + OB + OC)(OA + OB - OC)(OA - OB + OC)(-OA + OB + OC)/4}$

15: $\theta_{OB} = \arcsin(\frac{3 \cdot V \cdot OB}{2S^2})$

16: $\theta_{AOB} = \arcsin((b_2 + a_2 - c_2)/(2 \cdot OB \cdot OA))$

17: $\theta_{ABO} = \arcsin((b_2 + c_2 - a_2)/(2 \cdot OB \cdot OC))$

18: $A_{local.x} = OA \cdot \cos(\theta_{AOB})$

19: $A_{local.y} = OA \cdot \sin(\theta_{AOB})$

20: $B_{local.x} = OB$

21: $C_{local.x} = OC \cdot \cos(\theta_{ABO})$

22: $C_{local.y} = OC \cdot \sin(\theta_{ABO})$

23: $A_{local} = [A_{local.x}, A_{local.y}, 0]$

24: $B_{local} = [B_{local.x}, 0, 0]$

25: $C_{local} = [C_{local.x}, C_{local.y}, 0]$

26: $O_{local} = [0, 0, 0]$

27: $R = \begin{bmatrix} 1 & 0 & 0 \\ 0 & \cos(\theta_{OB}) & -\sin(\theta_{OB}) \\ 0 & \sin(\theta_{OB}) & \cos(\theta_{OB}) \end{bmatrix}$

28: $T_{rot} = (R, 0)$

29: $C_{local} = T_{rot} \circ C_{local}$

30: $O_g = T_g \circ O_{local}$

31: $A_g = T_g \circ A_{local}$

32: $B_g = T_g \circ B_{local}$

33: $C_g = T_g \circ C_{local}$

34: $OA_2 = \frac{O_g + A_g}{2}$

35: $OB_2 = \frac{O_g + B_g}{2}$

36: $OC_2 = \frac{O_g + C_g}{2}$

37: $AB_2 = \frac{A_g + B_g}{2}$

38: $AC_2 = \frac{A_g + C_g}{2}$

39: $BC_2 = \frac{B_g + C_g}{2}$

40: $l_1 = [OA_2, BC_2]$

41: $l_2 = [OB_2, AC_2]$

42: $l_3 = [OC_2, AB_2]$

43: **return** l_1, l_2, l_3

Algorithm 11 Make predicted symmetry axes consistent in Dn symmetry

Input: C^α coordinate of base ASU p_0 , Symmetry axes l_1 , l_2 , Number of replicates n .

$\triangleright l_1, l_2 \in \mathbb{R}^{2 \times 3}$

Output: Symmetry axes l_3, l_4 .

$\triangleright l_3, l_4 \in \mathbb{R}^{2 \times 3}$

def SymmetryAxisIso2(p_0, l_1, l_2, n)

- 1: $l_3 = \text{ApplySymmetryOp}(l_1, l_2, 2)$
 - 2: $l_4 = \text{ApplySymmetryOp}(l_2, l_1, 2)$
 - 3: $p_1 = \text{ApplySymmetryOp}(p_0, l_1, 2)$
 - 4: $p_2 = \text{ApplySymmetryOp}(p_0, l_2, 2)$
 - 5: $p_3 = \text{ApplySymmetryOp}(p_1, l_4, 2)$
 - 6: $p_4 = \text{ApplySymmetryOp}(p_2, l_3, 2)$
 - 7: $l_5 = \text{SymmetryAxisHeterologous}(p_0, p_3, p_4, n/2)$
 - 8: $c_0 = \text{mean}(p_0)$
 - 9: $c_1 = \text{mean}(p_1)$
 - 10: $c_2 = \text{mean}(p_2)$
 - 11: **if** $\|c_0 - c_1\| < \|c_0 - c_2\|$ **then**
 - 12: $m = \frac{c_0 + c_1}{2}$
 - 13: **else**
 - 14: $m = \frac{c_0 + c_2}{2}$
 - 15: $e = \text{VecPoint2Line}(m, l_5)$
 - 16: $l_6 = [m, m + e]$
 - 17: **return** l_5, l_6
-

Algorithm 12 Dihedral symmetry generator

Input: Backbone frames \mathcal{T} , Confidence score map C , Nearest position map P^{nst} , Chain id map M , Number of selection K , Number of replicates n .

$\triangleright P^{nst} \in \mathbb{R}^{N \times N}$, $M \in \mathbb{R}^{7 \times N \times N}$, $C \in \mathbb{R}^{7 \times N \times N}$

Output: Atom positions of backbone p_{all} .

$\triangleright p_{all} \in \mathbb{R}^{n \times N \times 3 \times 3}$

def DihedralSymmetryGenerator($\mathcal{T}, P^{nst}, M, C, K, n$)

- 1: $p_{bb} := \text{backbone atom positions}$ $\triangleright p_{bb} \in \mathbb{R}^{N \times 3 \times 3}$
 - 2: $p_0 := C^\alpha \text{ position}$ $\triangleright p_0 \in \mathbb{R}^{N \times 3}$
 - 3: $S = \text{GetPointIndexSet}(M, C, K)$ $\triangleright S \in \mathbb{R}^{7 \times K \times 2}$
 - 4: $iso_2 = \sum S[1]$
 - 5: $hetero_2 = \sum S[3]$
 - 6: **if** $n == 4$ **then**
 - 7: $l_1 = \text{SymmetryAxisIsologous}(\mathcal{T}, P^{nst}, S[0])$
 - 8: $l_2 = \text{SymmetryAxisIsologous}(\mathcal{T}, P^{nst}, S[1])$
 - 9: $l_3 = \text{SymmetryAxisIsologous}(\mathcal{T}, P^{nst}, S[2])$
 - 10: $p_1 = \text{ApplySymmetryOp}(p_0, l_1, 2)$
 - 11: $p_2 = \text{ApplySymmetryOp}(p_0, l_2, 2)$
 - 12: $p_3 = \text{ApplySymmetryOp}(p_0, l_3, 2)$
 - 13: $l_1, l_2, l_3 = \text{SymmetryAxisIsosceles}(p_0, p_1, p_2, p_3)$
 - 14: $p_1 = \text{ApplySymmetryOp}(p_{bb}, l_1, 2)$
 - 15: $p_2 = \text{ApplySymmetryOp}(p_{bb}, l_2, 2)$
 - 16: $p_3 = \text{ApplySymmetryOp}(p_{bb}, l_3, 2)$
 - 17: $p_{all} = \text{concat}(p_{bb}, p_1, p_2, p_3)$
 - 18: **else if** $iso_2 > hetero_2$ **then**
 - 19: $l_1 = \text{SymmetryAxisIsologous}(\mathcal{T}, P^{nst}, S[0])$
 - 20: $l_2 = \text{SymmetryAxisIsologous}(\mathcal{T}, P^{nst}, S[1])$
 - 21: $p_1 = \text{ApplySymmetryOp}(p_0, l_1, 2)$
 - 22: $p_2 = \text{ApplySymmetryOp}(p_0, l_2, 2)$
 - 23: $l_1, l_2 = \text{SymmetryAxisIso2}(p_0, l_1, l_2, n)$
 - 24: $p_2 = \text{ApplySymmetryOp}(p_{bb}, l_1, n/2)$
 - 25: $p_{all} = \text{ApplySymmetryOp}(p_2, l_2, 2)$
 - 26: **else**
 - 27: $p_1 = \text{ReconstructNeighbourChain}(\mathcal{T}, P^{nst}, S[3])$
 - 28: $p_2 = \text{ReconstructNeighbourChain}(\mathcal{T}, P^{nst}, S[4])$
 - 29: $l_1 = \text{SymmetryAxisHeterologous}(p_0, p_1, p_2)$
 - 30: $l_2 = \text{SymmetryAxisIsologous}(\mathcal{T}, P^{nst}, S[0])$
 - 31: $p_2 = \text{ApplySymmetryOp}(p_{bb}, l_1, n/2)$
 - 32: $p_{all} = \text{ApplySymmetryOp}(p_2, l_2, 2)$
 - 33: **return** p_{all}
-

Algorithm 13 Generate the whole assembly by interfaces for tetrahedral symmetry

Input: Atom positions of base ASU backbone p_{bb} , symmetry axes l_1, l_2, l_5 , number of replicates n .

$$\triangleright p_{bb} \in \mathbb{R}^{N \times 3 \times 3}, l_1, l_2, l_5 \in \mathbb{R}^{2 \times 3}$$

Output: Atom positions of backbone p_{all} .

$$\triangleright p_{all} \in \mathbb{R}^{n \times N \times 3 \times 3}$$

def ApplyTetrahedralSymmetry(p_{bb}, l_1, l_2, l_5)

```
1:  $c_1 = \text{mean}(p_{bb}[:, 1, :])$ 
2:  $c_1, c_2, c_3 = \text{ApplySymmetryOp}(c_1, l_1, 3)$ 
3:  $c_{123} = \text{Concat}(c_1, c_2, c_3)$ 
4: if  $l_2 \neq \text{None}$  then
5:    $a_{12} = ((l_1[: 3] - l_1[3 :])^T (l_2[: 3] - l_2[3 :]))$ 
6:    $c_{123}, c_{456}, c_{789} = \text{ApplySymmetryOp}(c_{123}, l_2, 3)$ 
7:    $p_1, p_2, p_3 = \text{mean}(c_{123}), \text{mean}(c_{456}), \text{mean}(c_{789})$ 
8:    $d = \|p_1 - p_2\|$ 
9:    $u_n = l_1[: 3] - l_1[3 :]$ 
10:   $u_n = \frac{u_n}{\|u_n\|}$ 
11:   $c = p_1 + \sqrt{\frac{2}{3}} \cdot d \cdot u_n$ 
12:   $v_2, v_3 = p_2 - c, p_3 - c$ 
13:   $v_2, v_3 = v_2 - v_2^T u_n \cdot u_n, v_3 - v_3^T u_n \cdot u_n$ 
14:   $v_2, v_3 = \frac{v_2}{\|v_2\|} \cdot \frac{\sqrt{3}}{3} \cdot d, \frac{v_3}{\|v_3\|} \cdot \frac{\sqrt{3}}{3} \cdot d$ 
15:   $v_4 = -v_2 - v_3$ 
16:   $v_4 = \frac{v_4}{\|v_4\|} \cdot \frac{\sqrt{3}}{3} \cdot d$ 
17:   $p_4 = c + v_4$ 
18:   $T_{rot} = \text{Frame3Points}(l_1[: 3], c, p_4)$ 
19:   $v_{4n} = \|v_4\|$ 
20:   $p_{2,local} = [0, -v_{4n}/2, \sqrt{3}/2 \cdot v_{4n}]$ 
21:   $p_{3,local} = [0, -v_{4n}/2, -\sqrt{3}/2 \cdot v_{4n}]$ 
22:   $p_2, p_3 = T_{rot} \circ p_{2,local}, T_{rot} \circ p_{3,local}$ 
23: else
24:   $c_{123}, c_{456} = \text{ApplySymmetryOp}(c_{123}, l_5, 2)$ 
25:   $p_1 = \text{mean}(c_{123})$ 
26:   $p_2 = \text{mean}(c_{456})$ 
27:   $d = \|p_1 - p_2\|$ 
28:   $u_n = l_1[: 3] - l_1[3 :]$ 
29:   $u_n = \frac{u_n}{\|u_n\|}$ 
30:   $c = p_1 + \sqrt{\frac{2}{3}} \cdot d \cdot u_n$ 
31:   $v_2 = p_2 - c$ 
32:   $v_2 = v_2 - v_2^T u_n \cdot u_n$ 
33:   $T_{rot} = \text{Frame3Points}(l_1[: 3], c, p_4)$ 
34:   $v_{2n} = \|v_2\|$ 
35:   $p_{3,local} = [0, -v_{2n}/2, \sqrt{3}/2 \cdot v_{2n}]$ 
36:   $p_{4,local} = [0, -v_{2n}/2, -\sqrt{3}/2 \cdot v_{2n}]$ 
37:   $p_3, p_4 = T_{rot} \circ p_{3,local}, T_{rot} \circ p_{4,local}$ 
38:   $v_0, v_1, v_2, v_3, v_4 = p_1, p_2, p_3, p_4$ 
39:   $m_1, m_2, m_3 = \frac{v_0+v_1}{2}, \frac{v_0+v_2}{2}, \frac{v_0+v_3}{2}$ 
40:   $m_{12}, m_{23}, m_{13} = \frac{v_1+v_2}{2}, \frac{v_2+v_3}{2}, \frac{v_1+v_3}{2}$ 
41:   $r_0 = [\frac{v_1+v_2+v_3}{3}, v_0]$ 
42:   $r_1, r_2, r_3 = [m_1, m_{23}], [m_2, m_{13}], [m_3, m_{12}]$ 
43:   $p_{bb} = \text{ApplySymmetryOp}(p_{bb}, r_0, 3)$ 
44:   $p_1 = \text{ApplySymmetryOp}(p_{bb}, r_1, 2)$ 
45:   $p_2 = \text{ApplySymmetryOp}(p_{bb}, r_2, 2)$ 
46:   $p_3 = \text{ApplySymmetryOp}(p_{bb}, r_3, 2)$ 
47:   $p_{all} = \text{concat}(p_{bb}, p_1, p_2, p_3)$ 
48: return  $p_{all}$ 
```

Algorithm 14 Tetrahedral symmetry generator

Input: Backbone frames \mathcal{T} , Confidence score map C , Nearest position map P^{nst} , Chain id map M , Number of selection K , Number of replicates n .

$$\triangleright P^{nst} \in \mathbb{R}^{N \times N}, M \in \mathbb{R}^{7 \times N \times N}, C \in \mathbb{R}^{7 \times N \times N}$$

Output: Atom positions of backbone p_{all} .

$\triangleright p_{all} \in \mathbb{R}^{n \times N \times 3 \times 3}$

```
def TetrahedralSymmetryGenerator( $\mathcal{T}, P^{nst}, M, C, K, n$ )
1:  $p_{bb} :=$  backbone atom positions  $\triangleright p_{bb} \in \mathbb{R}^{N \times 3 \times 3}$ 
2:  $p_0 := C^\alpha$  position  $\triangleright p_0 \in \mathbb{R}^{N \times 3}$ 
3:  $S = \text{GetPointIndexSet}(M, C, K)$   $\triangleright S \in \mathbb{R}^{7 \times K \times 2}$ 
4:  $iso_2 = \sum S[1]$ 
5:  $hetero_2 = \sum S[5]$ 
6: if  $iso_2 > hetero_2$  then
7:    $l_1 = \text{SymmetryAxisIsologous}(\mathcal{T}, P^{nst}, S[0])$ 
8:    $l_2 = \text{SymmetryAxisIsologous}(\mathcal{T}, P^{nst}, S[1])$ 
9:    $p_1 = \text{ApplySymmetryOp}(p_0, l_1, 2)$ 
10:   $p_2 = \text{ApplySymmetryOp}(p_0, l_2, 2)$ 
11:   $l_1, l_2 = \text{SymmetryAxisIso2}(p_0, l_1, l_2, n)$ 
12:   $p_{all} = \text{ApplyTetrahedralSymmetry}(p_{bb}, l_1, None, l_2)$ 
13: else
14:   $p_1 = \text{ReconstructNeighbourChain}(\mathcal{T}, P^{nst}, S[3])$ 
15:   $p_2 = \text{ReconstructNeighbourChain}(\mathcal{T}, P^{nst}, S[4])$ 
16:   $l_1 = \text{SymmetryAxisHeterologous}(p_0, p_1, p_2)$ 
17:   $p_3 = \text{ReconstructNeighbourChain}(\mathcal{T}, P^{nst}, S[5])$ 
18:   $p_4 = \text{ReconstructNeighbourChain}(\mathcal{T}, P^{nst}, S[6])$ 
19:   $l_2 = \text{SymmetryAxisHeterologous}(p_0, p_3, p_4)$ 
20:   $p_{all} = \text{ApplyTetrahedralSymmetry}(p_{bb}, l_1, l_2, None)$ 
21: return  $p_{all}$ 
```

Algorithm 15 Generate the whole assembly by interfaces for octahedral symmetry

Input: Atom positions of base ASU backbone p_{bb} , symmetry axes l_1, l_2 , number of replicates n .

$$\triangleright p_{bb} \in \mathbb{R}^{N \times 3 \times 3}, l_1, l_2 \in \mathbb{R}^{2 \times 3}$$

Output: Atom positions of backbone p_{all} .

$$\triangleright p_{all} \in \mathbb{R}^{n \times N \times 3 \times 3}$$

```
def ApplyOctahedralSymmetry( $p_{bb}, l_1, l_2$ )
1:  $c = \text{CrossPoint}(l_1, l_2)$ 
2:  $r_2 = (l_2[3:] - l_2[:3]) \times (l_1[3:] - l_1[:3])$ 
3:  $r_2 = [c, r_2 + c]$ 
4:  $c_3 = \text{ApplySymmetryOp}(p_{bb}, l_2, 3)$ 
5:  $c_{12} = \text{ApplySymmetryOp}(c_3, l_1, 4)$ 
6:  $c_{24} = \text{ApplySymmetryOp}(c_{12}, r_2, 2)$ 
7:  $p_{all} = c_{24}$ 
8: return  $p_{all}$ 
```

Algorithm 16 Octahedral symmetry generator

Input: Backbone frames \mathcal{T} , Confidence score map C , Nearest position map P^{nst} , Chain id map M , Number of selection K , Number of replicates n .

$$\triangleright P^{nst} \in \mathbb{R}^{N \times N}, M \in \mathbb{R}^{7 \times N \times N}, C \in \mathbb{R}^{7 \times N \times N}$$

Output: Atom positions of backbone p_{all} .

$$\triangleright p_{all} \in \mathbb{R}^{n \times N \times 3 \times 3}$$

```
def OctahedralSymmetryGenerator( $\mathcal{T}, P^{nst}, M, C, K, n$ )
1:  $p_{bb} :=$  backbone atom positions  $\triangleright p_{bb} \in \mathbb{R}^{N \times 3 \times 3}$ 
2:  $p_0 := C^\alpha$  position  $\triangleright p_0 \in \mathbb{R}^{N \times 3}$ 
3:  $S = \text{GetPointIndexSet}(M, C, K)$   $\triangleright S \in \mathbb{R}^{7 \times K \times 2}$ 
4:  $p_1 = \text{ReconstructNeighbourChain}(\mathcal{T}, P^{nst}, S[3])$ 
5:  $p_2 = \text{ReconstructNeighbourChain}(\mathcal{T}, P^{nst}, S[4])$ 
6:  $l_1 = \text{SymmetryAxisHeterologous}(p_0, p_1, p_2)$ 
7:  $p_3 = \text{ReconstructNeighbourChain}(\mathcal{T}, P^{nst}, S[5])$ 
8:  $p_4 = \text{ReconstructNeighbourChain}(\mathcal{T}, P^{nst}, S[6])$ 
9:  $l_2 = \text{SymmetryAxisHeterologous}(p_0, p_3, p_4)$ 
10:  $p_{all} = \text{ApplyOctahedralSymmetry}(p_{bb}, l_1, l_2)$ 
11: return  $p_{all}$ 
```

Algorithm 17 Generate the whole assembly by interfaces for icosahedral symmetry

Input: Atom positions of base ASU backbone p_{bb} , symmetry axes l_1, l_2, l_5 , number of replicates n .

$$\triangleright p_{bb} \in \mathbb{R}^{N \times 3 \times 3}, l_1, l_2, l_5 \in \mathbb{R}^{2 \times 3}$$

Output: Atom positions of backbone p_{all} .

$$\triangleright p_{all} \in \mathbb{R}^{n \times N \times 3 \times 3}$$

```
def ApplyIcosahedralSymmetry( $p_{bb}, l_5, l_3, l_2$ )
1:  $r_{2s} = l_2[:3]$ 
2:  $r_{2e} = l_2[3:]$ 
3:  $r12_{2s} = \text{ApplySymmetryOp}(r_{2s}, l_3, 3)$ 
4:  $r12_{2e} = \text{ApplySymmetryOp}(r_{2e}, l_3, 3)$ 
5:  $r2_1 = [r12_{2s}[1], r12_{2e}[1]]$ 
6:  $r2_2 = [r12_{2s}[2], r12_{2e}[2]]$ 
7:  $\theta_1 = \text{Angle}(r2_1, l_5)$ 
8:  $\theta_2 = \text{Angle}(r2_2, l_5)$ 
9:
10: if  $\theta_1 \geq \theta_2$  then
11:    $r_v = r2_1$ 
12:
13: else
14:    $r_v = r2_2$ 
15:
16:  $c = \text{CrossPoint}(l_5, l_3)$ 
17:  $r_2 = (l_5[3:] - l_5[:3]) \times (l_3[3:] - l_3[:3])$ 
18:  $r_2 = [c, r_2 + c]$ 
19:  $c_3 = \text{ApplySymmetryOp}(p_{bb}, l_3, 3)$ 
20:  $c_6 = \text{ApplySymmetryOp}(c_3, r_v, 2)$ 
21:  $c_{30} = \text{ApplySymmetryOp}(c_6, l_5, 5)$ 
22:  $c_{60} = \text{ApplySymmetryOp}(c_{30}, r_2, 2)$ 
23:  $p_{all} = c_{60}$ 
24: return  $p_{all}$ 
```

Algorithm 18 Icosahedral symmetry generator

Input: Backbone frames \mathcal{T} , Confidence score map C ,
Nearest position map P^{nst} , Chain id map M , Number
of selection K , Number of replicates n .

▷ $P^{nst} \in \mathbb{R}^{N \times N}$, $M \in \mathbb{R}^{7 \times N \times N}$, $C \in \mathbb{R}^{7 \times N \times N}$

Output: Atom positions of backbone p_{all} .

▷ $p_{all} \in \mathbb{R}^{n \times N \times 3 \times 3}$

def IcosahedralSymmetryGenerator(\mathcal{T} , P^{nst} , M , C , K , n)

- 1: $p_{bb} :=$ backbone atom positions ▷ $p_{bb} \in \mathbb{R}^{N \times 3 \times 3}$
 - 2: $p_0 := C^\alpha$ position ▷ $p_0 \in \mathbb{R}^{N \times 3}$
 - 3: $S =$ GetPointIndexSet(M , C , K) ▷ $S \in \mathbb{R}^{7 \times K \times 2}$
 - 4: $p_1 =$ ReconstructNeighbourChain(\mathcal{T} , P^{nst} , $S[3]$)
 - 5: $p_2 =$ ReconstructNeighbourChain(\mathcal{T} , P^{nst} , $S[4]$)
 - 6: $l_1 =$ SymmetryAxisHeterologous(p_0 , p_1 , p_2)
 - 7: $p_3 =$ ReconstructNeighbourChain(\mathcal{T} , P^{nst} , $S[5]$)
 - 8: $p_4 =$ ReconstructNeighbourChain(\mathcal{T} , P^{nst} , $S[6]$)
 - 9: $l_2 =$ SymmetryAxisHeterologous(p_0 , p_3 , p_4)
 - 10: $l_3 =$ SymmetryAxisIsologous(\mathcal{T} , P^{nst} , $S[0]$)
 - 11: $p_{all} =$ ApplyIcosahedralSymmetry(p_{bb} , l_1 , l_2 , l_3)
 - 12: **return** p_{all}
-